Radiative transfer equation for multiple diffraction

Emeline Reboul, Alain Le Bot,[a)] and Joël Perret-Liaudet
Laboratoire de Tribologie et Dynamique des Systèmes, École Centrale de Lyon, 36,
Avenue Guy de Collongue 69134 Ecully, France

This paper aims to apply the radiative transfer method to acoustical diffraction by obstacles. Some fictitious sources are introduced at diffracting wedges and a transfer equation based on energy balance determines the diffracted powers. It leads to a set of linear equations on diffracted powers which can be solved in a finite number of steps. It is then possible to calculate the diffracted field anywhere. Some applications to diffraction by obstacles of various shapes are presented. Results of this method are compared with Geometrical Theory of Diffraction and BEM reference calculations. It is shown that this method is particularly efficient in case of multiple diffraction where the ray-tracing technique involves an infinite number of rays between a source and a receiver point. © 2005 Acoustical Society of America. [DOI: 10.1121/1.2001467]

LIST OF SYMBOLS

$$
\begin{aligned}
\gamma_0 &= \text{solid angle of space;} \\
\Omega &= \text{acoustical domain;} \\
\Gamma &= \text{surface of } \Omega; \\
\Delta &= \text{set of diffracting points of } \Gamma; \\
c &= \text{speed of sound;} \\
m &= \text{attenuation factor;} \\
W &= \text{energy density;} \\
\mathbf{I} &= \text{intensity vector;} \\
G &= \text{energy density of direct field;} \\
\mathbf{H}, H &= \text{intensity of direct field, magnitude;} \\
D_\omega &= \text{energetic coefficient of diffraction;} \\
\rho &= \text{magnitude of actual sources;} \\
\sigma &= \text{magnitude of diffraction sources;} \\
\mathbf{u}, \theta, \alpha &= \text{emission direction, emission angles;} \\
\mathbf{v}, \varphi, \beta &= \text{incidence direction, incidence angles;} \\
\mathbf{s} &= \text{source point;} \\
\mathbf{r} &= \text{receiver point;} \\
\mathbf{p}, \mathbf{q} &= \text{diffraction point.}
\end{aligned}
$$

I. INTRODUCTION

The Geometrical Theory of Diffraction (GTD), stated by Keller[1] in the 1960s, leads to an elegant description of diffraction in terms of rays. Starting from a generalized Fermat's principle, GTD states the existence of diffracted rays by wedges and peaks, creeping rays, and many others in addition to the classical direct and reflected rays of geometrical optics. It is then possible to predict the field in the shadow zone of obstacles in a simple way, provided that all paths from the source to the receiver point are listed. The field at the receiver point is simply the sum of all the fields attached to individual rays.

GTD has been successfully applied in acoustics for the problem of single-edge diffraction[2,3] and all problems of diffraction around corners such as buildings or the top of the

noise barriers. When the diffracting structure has more than one point of diffraction, waves can be diffracted at each point more than once. This is referred to as multiple diffraction, and can lead to an unlimited number of possible paths for diffracted rays. Pierce[4] gives an approximate expression for double-edge diffraction by a thick, three-sided barrier based on concepts inherent to the GTD. His formulation is particularly well suited for convex-shaped edges, small angles of diffraction, and when the width of the barrier exceeds one wavelength. It was used by Kurze[5] to assess the efficiency of wide barriers. The work of Medwin *et al.*[6] is dedicated to double diffraction in the time domain and is applicable to any multiple diffraction. The technique consists in introducing an infinite number of infinitesimal sources at the first edge, each of which spawns an infinite number of diffractions at the second edge. This method is applied by Ouis[7] to improve the evaluation of the insertion loss of a hard wedged barrier. The multiple diffraction, up to second order, between the top of the wedge barrier and its base is considered. In the same context, Jin *et al.*[8] predict the insertion loss of partially inclined noise barriers considering multiple diffraction occurring at convex as well as concave edges. Formulations for single to triple diffracted waves are constructed based on Kouyoumjian and Pathak's diffraction theory.[9] They show that including additional diffraction at edges improves GTD by removing many small oscillations in the frequency domain. In any case, all these methods take into account a finite number of diffraction order. GTD is particularly well suited in cases where the number of paths is limited or, at least, where all paths can be clearly identified. But, in all other cases, the determination of all source-receiver paths may lead to unsuspected difficulties.

There exists another way to present geometrical acoustics: the so-called "standard procedure" or factor view method in radiative transfer.[10] It is based on a transfer equation which states the equilibrium of energy exchange between two facing surfaces. All rays traveling between these two surfaces, including infinitely reflected ones, are taken into account in the form of an integral equation.

[a)]Electronic mail: alain.le-bot@ec-lyon.fr

In acoustics, an application of this method leads to the so-called "radiosity method,"[11–14] which aims at the prediction of reverberation time beyond the validity of Sabine's formula. Applied to the determination of SPL in rooms,[15] vibrational levels in built-up structures[16] or radiation of sound,[17] the radiative transfer approach provides an alternative to both the ray-tracing technique in room acoustics and the statistical energy analysis in vibroacoustics. Related works based on an energy approach include for room acoustics[18] and for noise radiated by structures.[19]

This paper aims to generalize the radiosity method to account for diffraction, that is, to establish the transfer equation for diffraction sources. However, this study is limited to diffraction by wedges and peaks. Diffraction by smooth objects such as cylinders involves creeping waves that are not included in this work. For wedges and peaks, some fictitious diffraction sources are introduced at diffracting vertices. The total diffracted power of these sources is the sum of the diffracted powers of the individual rays. The transfer equation for diffraction sources is established. In some cases of multiple diffraction, i.e., where several diffraction sources interact, it reduces to a linear set of equations on power of diffraction sources. It is then possible to determine the diffracted powers and so, the energy field in the whole acoustical domain. This method allows the solving of multiple diffraction problems in a finite number of steps, to be compared with the infinite number of rays needed in the classical ray-tracing approach. Some results have been published[20] in a short note but limited to the particular two-dimensional case. In this paper, the development of the method is completely detailed including the three-dimensional case.

The outline of the present paper is as follows. In Sec. II all the theoretical material is presented, fictitious diffraction sources are introduced, and the transfer equation which determines their magnitude is derived from power balance. In Sec. III, the transfer equation is solved in the case of a plane wave incident on a three-dimensional wedge, and it is shown that it is consistent with the classical solution of GTD. The diffraction by double wedges is dealt with in Sec. IV. This example highlights the method for solving the transfer equation and the difference with classical ray-tracing algorithms of GTD. A more elaborate example is developed in Sec. V to assess the power of the method.

II. RADIATIVE TRANSFER EQUATION

Let us denote by G the energy density attached to the direct field and by $\mathbf{H}$ the intensity field. Expressions for direct fields depend only on the dimension of the wave but not on the kind of system. For instance, the decrease of energy of a circular wave is the same in vibrating plates and on liquid surfaces. The following expressions are valid for any isotropic and homogeneous medium:

$$G(\mathbf{s},\mathbf{r}) = \frac{1}{\gamma_0 c} \frac{e^{-ms}}{s^{n-1}}, \tag{1}$$

$$\mathbf{H}(\mathbf{s},\mathbf{r}) = \frac{1}{\gamma_0} \frac{e^{-ms}}{s^{n-1}} \mathbf{u}, \tag{2}$$

where $\gamma_0=2$ and $n=1$ for plane waves, $\gamma_0=2\pi$ and $n=2$ for cylindrical waves, and $\gamma_0=4\pi$ and $n=3$ for spherical waves. c is the group speed, $s=|\mathbf{s}-\mathbf{r}|$ the source-receiver distance, and m is the attenuation factor to account for the decrease of wave magnitude when traveling. $H=cG$ denotes the magnitude of intensity vector $\mathbf{H}$, and sometimes, for the sake of brievety, $G(\mathbf{s},\mathbf{r})$ and $H(\mathbf{s},\mathbf{r})$ will be denoted $G(s)$ and $H(s)$ with $s=|\mathbf{s}-\mathbf{r}|$.

In some cases, an obstacle located between the source and the receiver can stop the direct field. The receiver is not affected by the direct field, but can be affected by some reflected or diffracted fields. It is then convenient to introduce a visibility function $V(\mathbf{s},\mathbf{r})$ equal to 1 when $\mathbf{r}$ is visible from $\mathbf{s}$ and 0 otherwise. Final expressions for direct field are

$$G(\mathbf{s},\mathbf{r}) = V(\mathbf{s},\mathbf{r}) \frac{1}{\gamma_0 c} \frac{e^{-ms}}{s^{n-1}}, \tag{3}$$

$$\mathbf{H}(\mathbf{s},\mathbf{r}) = V(\mathbf{s},\mathbf{r}) \frac{1}{\gamma_0} \frac{e^{-ms}}{s^{n-1}} \mathbf{u}. \tag{4}$$

Thus, direct field is equal to zero in shadow zones of obtacles.

Now, consider the field in a domain Ω induced by some distributed actual sources $\mathbf{s}$ of power density ρ. The direct field is simply the superposition of all individual direct fields, that is, $\int \rho G d\Omega$ where $d\Omega$ is the Lebesgue measure in Ω. Furthermore, waves when traveling are reflected by the surface Γ of the domain and also diffracted by all wedges, peaks, and more generally all singularities of the surface Γ. The set of all diffracting lines is denoted Δ_1 while the set of all diffracting vertices is denoted Δ_0. Some fictitious sources are introduced at all these points where something occurs to incident waves. The power of these fictitious sources is denoted by σ, which may depend on the position of the source but also on the emission direction and time for time-varying problems. In any case, the field radiated by these sources is $\int \sigma G d\Gamma$ for reflection, $d\Gamma$ being the surface measure on Γ, $\int \sigma G d\Delta$ for diffraction by wedges, $d\Delta$ being the length measure on Δ_1 and $\Sigma \sigma G$ for diffraction by peaks, the sum running over the set Δ_0 of all diffracting peaks. Finally, the complete field at any point is obtained by adding the contributions of all types of sources. Therefore, the energy density is at any $\mathbf{r} \in \Omega$ and at time t,

$$W(\mathbf{r},t) = \int_\Omega \rho(\mathbf{s},t-s/c)G(\mathbf{s},\mathbf{r})d\Omega_{\mathbf{s}} + \int_\Gamma \sigma(\mathbf{p},\mathbf{u},t$$
$$- r/c)G(\mathbf{p},\mathbf{r})d\Gamma_{\mathbf{p}} + \int_{\Delta_1} \sigma(\mathbf{p},\mathbf{u},t$$
$$- r/c)G(\mathbf{p},\mathbf{r})d\Delta_{\mathbf{p}} + \sum_{\mathbf{p}\in\Delta_0} \sigma(\mathbf{p},\mathbf{u},t-r/c)G(\mathbf{p},\mathbf{r}), \tag{5}$$

and the intensity is

$$\mathbf{I}(\mathbf{r},t) = \int_\Omega \rho(\mathbf{s},t-s/c)\mathbf{H}(\mathbf{s},\mathbf{r})d\Omega_\mathbf{s} + \int_\Gamma \sigma(\mathbf{p},\mathbf{u},t$$

$$-r/c)\mathbf{H}(\mathbf{p},\mathbf{r})d\Gamma_\mathbf{p} + \int_{\Delta_1} \sigma(\mathbf{p},\mathbf{u},t$$

$$-r/c)\mathbf{H}(\mathbf{p},\mathbf{r})d\Delta_\mathbf{p} + \sum_{\mathbf{p}\in\Delta_0} \sigma(\mathbf{p},\mathbf{u},t-r/c)\mathbf{H}(\mathbf{p},\mathbf{r}),$$

$$(6)$$

where $s=|\mathbf{r}-\mathbf{s}|$ and $r=|\mathbf{r}-\mathbf{p}|$. $\mathbf{u}$ is the unit vector from the source point $\mathbf{s}$ or $\mathbf{p}$ to the receiver point $\mathbf{r}$ and r/c (or s/c) is the time delay for the propagation of energy from the source point to the receiver point.

Let us turn to the determination of the unknown σ. On the surface Γ where reflection occurs, several reflection laws can be adopted. The case of diffuse reflection has been developed in Ref. 15 and leads to an integral equation on the potential σ which has been solved using a collocation method. Otherwise, a specular law of reflection leads to a functional equation on σ.[21] In all cases where it works, the method of image sources provides a solution of this functional equation.

Consider now the case of diffraction. $D_\omega(\mathbf{v},\mathbf{u})$ is an energetic diffraction coefficient depending on two variables, the incident direction $\mathbf{v}$ and the emission direction $\mathbf{u}$. The subscript ω is used to specify that this coefficient also depends on frequency. First, if σ belongs to Δ_0, the energetic coefficient of diffraction $D_\omega(\mathbf{v},\mathbf{u})$ is defined as the ratio of the emitted power $d\mathcal{P}_{\text{emit}}$ per unit solid angle du about $\mathbf{u}$ and the incident intensity I_{inc} stemming from $\mathbf{v}$,

$$D_\omega(\mathbf{v},\mathbf{u}) = \frac{1}{I_{\text{inc}}} \times \frac{d\mathcal{P}_{\text{emit}}}{du}. \qquad (7)$$

Second, when σ belongs to Δ_1, $D_\omega(\mathbf{v},\mathbf{u})$ is defined as the ratio of the emitted power $d\mathcal{P}_{\text{emit}}$ per unit solid angle du about $\mathbf{u}$ and per unit length $d\nu$ of the edge, and the incident intensity I_{inc} stemming from $\mathbf{v}$,

$$D_\omega(\mathbf{v},\mathbf{u}) = \frac{1}{I_{\text{inc}}} \times \frac{d\mathcal{P}_{\text{emit}}}{d\nu du}. \qquad (8)$$

When incident energy is distributed among all directions, the emitted power about $\mathbf{u}$ is the sum of contributions of incident intensities leading to the detailed energy balance,[22]

$$\frac{d\mathcal{P}_{\text{emit}}}{du} \text{ or } \frac{d\mathcal{P}_{\text{emit}}}{d\nu du} = \int D_\omega(\mathbf{v},\mathbf{u})I_{\text{inc}}(\mathbf{v},t)dv, \qquad (9)$$

where I_{inc} is the incident intensity impinging on the diffracting point $\mathbf{p}$ at time t and stemming from direct, reflected fields and the field diffracted by all other diffracting wedges.

On the other hand, at a distance ϵ of any diffraction point, the emitted intensity is σH, and therefore the flux crossing an infinitesimal solid angle is $d\mathcal{P}_{\text{emit}}=du\sigma H\epsilon^{n-1} = du\sigma e^{-m\epsilon}/\gamma_0$ with the limit $du\sigma/\gamma_0$ for small ϵ. Substitution in Eq. (9) then leads to
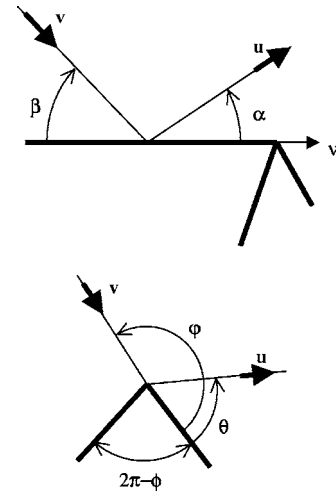
FIG. 1. Plane wave incident on a wedge with direction $\mathbf{v}$. The emission direction is denoted $\mathbf{u}$.

$$\frac{\sigma(\mathbf{p},\mathbf{u},t)}{\gamma_0} = \int_\Omega D_\omega(\mathbf{v},\mathbf{u})\rho(\mathbf{s},t-s/c)H(\mathbf{s},\mathbf{p})d\Omega_\mathbf{s}$$

$$+ \int_\Gamma D_\omega(\mathbf{v},\mathbf{u})\sigma(\mathbf{q},\mathbf{v},t-r/c)H(\mathbf{q},\mathbf{p})d\Gamma_\mathbf{q}$$

$$+ \int_{\Delta_1} D_\omega(\mathbf{v},\mathbf{u})\sigma(\mathbf{q},\mathbf{v},t-r/c)H(\mathbf{q},\mathbf{p})d\Delta_\mathbf{q}$$

$$+ \sum_{\mathbf{q}\in\Delta_0} D_\omega(\mathbf{v},\mathbf{u})\sigma(\mathbf{q},\mathbf{v},t-r/c)H(\mathbf{q},\mathbf{p}). \qquad (10)$$

This is a functional equation on the unknown σ for both Δ_0 and Δ_1. Once the potential σ is known, the field at any receiver point $\mathbf{r}$ is determined by applying Eqs. (5) and (6).

III. DIFFRACTION BY WEDGE

In this section, the problem of a steady-state plane wave diffracted by a wedge is solved using the method exposed in Sec. II. The aim is to check whether the energy solution agrees well with the classical GTD analysis in terms of rays. So, consider a plane wave of intensity I_{inc} impinging on a wedge with incidence $\mathbf{v}=\varphi,\beta$ as shown in Fig. 1. The edge of the wedge is along the ν axis. The outer angle of the wedge is denoted ϕ. For any emission direction $\mathbf{u}=\theta,\alpha$, the diffracted potential σ is given by Eq. (10) where the right-hand side reduces to the direct field term, i.e., the first integral,

$$\frac{\sigma(\nu,\theta,\alpha)}{4\pi} = D_\omega(\varphi,\beta;\theta,\alpha)I_{\text{inc}}. \qquad (11)$$

It is well known that all energy with incidence β is diffracted into a cone of axis the edge of the wedge and of half-angle β. This is the so-called Keller's cone. The bidirectional energetic coefficient of diffraction $D_\omega(\varphi,\beta;\theta,\alpha)$ then reduces to the particular form,

$$D_\omega(\varphi,\beta;\theta,\alpha) = D_\omega(\varphi,\theta)\delta(\alpha-\beta). \qquad (12)$$

It is found in the Appendix that $D_\omega(\varphi,\theta)=|d(\varphi,\theta)|^2$ is the energetic coefficient of diffraction at normal incidence,
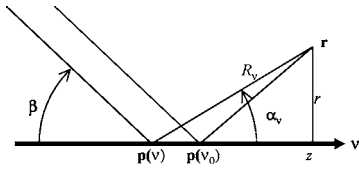
FIG. 2. The emission angle α_ν depends on the receiver point **r**. There is a single point $\mathbf{p}(\nu_0)$ where the emission angle equals the incidence angle β.

$d(\varphi, \theta)$ being the classical diffraction coefficient used in GTD. The energetic diffraction coefficient remains unchanged when incidence and emission directions are interchanged following the reciprocity principle,

$$D_\omega(\varphi, \theta) = D_\omega(\theta, \varphi). \tag{13}$$

Furthermore, the symmetry with respect to the medium plan of the wedge implies that the coefficient is invariant under the change of angle $\zeta \to \phi - \zeta$,

$$D_\omega(\varphi, \theta) = D_\omega(\phi - \varphi, \phi - \theta). \tag{14}$$

Now, introducing Eqs. (11) and (12) into the third integral of Eq. (5) leads to the diffracted energy at any point **r** $= r, \theta, z$ in cylindrical coordinates centered on the ν axis,

$$W_{\mathrm{dif}} = \int_{-\infty}^{\infty} \sigma(\nu, \theta, \alpha_\nu) G(\mathbf{p}, \mathbf{r}) d\nu$$

$$= \frac{I_{\mathrm{inc}}}{c} \int_{-\infty}^{\infty} D_\omega(\varphi, \theta) \delta(\alpha_\nu - \beta) \frac{d\nu}{R_\nu^2}, \tag{15}$$

where θ, α_ν are the emission angles at point **p** of coordinate ν on the edge toward **r** and R_ν is the distance between **p** and **r**. To evaluate this last integral, the following result of the theory of distributions is used;

$$\int g(x) \delta[f(x)] dx = \sum_i \frac{g(x_i)}{|f'(x_i)|}, \tag{16}$$

where the sum runs over all zeros of f included in the range of integration. It is found that the function $f(\nu) = \alpha_\nu - \beta$ $= \arctan[r/(z-\nu)] - \beta$ has a single zero $\nu_0 = z - r / \tan \beta$ which corresponds to the unique point for which emission angle α_0 toward **r** equals the incidence angle β (Fig. 2). Then,

$$f'(\nu_0) = \frac{d\alpha_\nu}{d\nu} = \frac{1}{1 + \frac{r^2}{(z-\nu)^2}} \times \frac{d}{d\nu} \left(\frac{r}{z-\nu} \right) = \frac{r}{R_\nu^2}. \tag{17}$$

Finally, the diffracted energy is

$$W_{\mathrm{dif}} = \frac{I_{\mathrm{inc}}}{c} D_\omega(\varphi, \theta) \times \frac{1}{r}, \tag{18}$$

that is, the energy is inversely proportional to the wedge-receiver distance r. The decrease of the energy of the field like $1/r$ well agrees with the decrease of the magnitude of the field like $1/\sqrt{r}$ predicted by GTD.[2]

A numerical simulation is proposed to compare the results given by the radiative transfer method to those given by the GTD. The edge outer angle is $\phi = 7\pi/4$ rad. An incident plane wave hits the wedge and gives rise to a reflected wave, a diffracted wave, and a surface ray propagating along the
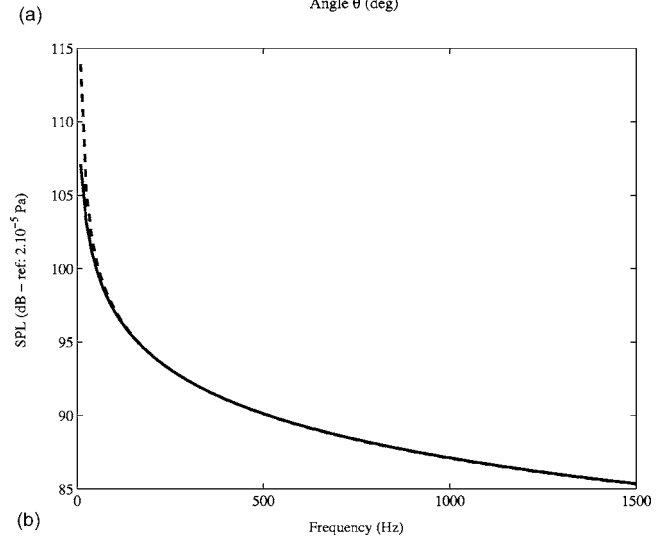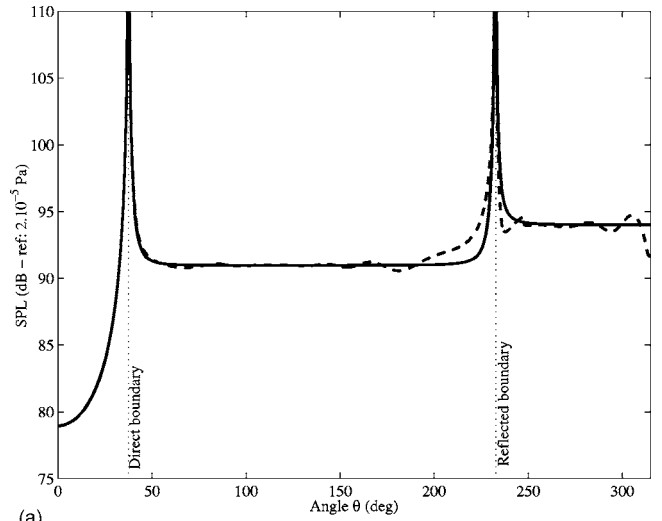
FIG. 3. Diffraction by a wedge of a plane wave with incidence $\varphi = 217.5°$. (a) Comparison of the SPL vs θ at $r = 1.5$ m obtained from the radiative equation (—) and GTD (---). The frequency is 1.5 kHz. The boundaries of direct field and diffracted field are, respectively, $\theta = \varphi - \pi$ and $\theta = 2\phi - \varphi - \pi$. (b) Comparison of the SPL vs frequency at $r = 1.5$ m and $\theta = 27.5°$ obtained from the radiative equation (—) and GTD (---). The receiver point is in the shadow area.

wedge. The receiver point is assumed to be far enough from the edge so that surface rays can be neglected. Two results are shown in Fig. 3. On the one hand, the behavior of the acoustical field around the wedge, at a constant distance r $= 1.5$ m from the edge, is represented in a plane perpendicular to the edge of the wedge. The frequency is 1.5 kHz. The incident direction is $\varphi = 217.5°$ from the right side of the wedge, $\beta = 40°$ (Fig. 1). In this problem, there are two boundary lines that, respectively, mark the transition from illumination to shadow for the incident field ($\theta = \varphi - \pi$) and for the reflected field ($\theta = 2\phi - \pi - \varphi$). GTD is known to fail near these geometrical boundaries, and so the radiative transfer method which uses the diffraction coefficient of the GTD also gives inaccurate results in these areas. Thus, both methods lead to similar results all around the wedge including these transition areas where they both lead to unphysical results. On the other hand, the same calculation is performed for a fixed position of the receiver point $r = 1.5$ m, $\theta = 27.5°$ in the shadow area of the wedge, but versus frequency. Both

Reboul, Le Bot, and Perret-Liaudet: Transfer equation for diffraction   1329
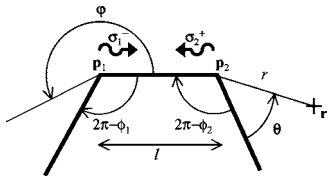
FIG. 4. Plane wave incident on a double wedge of width l with incidence angle φ. Two fictitious sources are located at $\mathbf{p}_1$ and $\mathbf{p}_2$.

methods are again in good agreement and show that the amplitude of the diffracted field decreases as the frequency increases.

IV. DIFFRACTION BY DOUBLE WEDGE

Let us now arrive to multiple diffraction. The simple case of double diffraction of a steady plane wave is solved by using GTD and Eq. (10). This example is chosen in order to illustrate similarities and differences of GTD and Eq. (10).

Consider a two-dimensional rigid three-sided barrier. An incident plane wave with intensity I_{inc} is impinging on the left-hand side, and one takes an interest in the evaluation of the energy density on the other side of the barrier. Let us introduce two fictitious diffraction sources at corners $\mathbf{p}_1$ and $\mathbf{p}_2$ of powers σ_1 and σ_2. The incidence angle φ and the emission θ are defined in Fig. 4. For the sake of simplicity, $\sigma_1(0)$ and $\sigma_2(\phi_2)$ are denoted σ_1^- and σ_2^+. Equations on σ_1^- and σ_2^+ are obtained by applying Eq. (10):

$$\frac{\sigma_1^-}{2\pi} = I_{\text{inc}}D_\omega(\varphi,0) + \sigma_2^+ H(l)D_\omega(0,0), \qquad (19)$$

$$\frac{\sigma_2^+}{2\pi} = \sigma_1^- H(l)D_\omega(\phi_2,\phi_2), \qquad (20)$$

where l is the width of the barrier, ϕ_i is the outer angle of corner $\mathbf{p}_i$. It has been assumed that the incident wave propagates upwards, i.e., $\varphi > \pi$. Otherwise a term for direct intensity must be added in the second equation. Applying again Eq. (10) leads to σ_2 at any emission angle θ,

$$\frac{\sigma_2(\theta)}{2\pi} = \sigma_1^- H(l)D_\omega(\phi_2,\theta). \qquad (21)$$

By using the relationship $D_\omega(\phi_2,\phi_2)=D_\omega(0,0)$ from Eq. (14), the solution of Eqs. (19) and (20) is

$$\sigma_1^- = I_{\text{inc}}\frac{2\pi D_\omega(\varphi,0)}{1 - 4\pi^2 H^2(l)D_\omega^2(0,0)}. \qquad (22)$$

And then,

$$\sigma_2(\theta) = I_{\text{inc}}\frac{4\pi^2 D_\omega(\varphi,0)H(l)D_\omega(\phi_2,\theta)}{1 - 4\pi^2 H^2(l)D_\omega^2(0,0)}. \qquad (23)$$

The field at any point $\mathbf{r}$ on the right side of the barrier below the top, i.e., $\theta < \phi_2 - \pi$ is given by Eq. (5) with the only contribution of the diffracted field from $\mathbf{p}_2$:

$$W(\mathbf{r}) = \sigma_2(\theta)G(r), \qquad (24)$$

where $r = |\mathbf{p}_2 - \mathbf{r}|$. Thus,

$$W(\mathbf{r}) = \frac{I_{\text{inc}}}{c}\frac{D_\omega(\varphi,0)D_\omega(\phi_2,\theta)}{1 - \dfrac{D_\omega^2(0,0)}{l^2}} \times \frac{1}{lr}, \qquad (25)$$

by assuming that the attenuation factor is zero, that is $H(l)=1/2\pi l$ and $G(r)=1/2\pi cr$. This expression for energy is valid under the condition that $D_\omega(0,0)/l < 1$.

Let us turn to the same problem by means of the GTD. The pressure p_2 at point $\mathbf{p}_2$ is determined by summing all contributions of rays arriving at this point and can be written as

$$p_2 = p_0 D_\omega(\varphi,0)\frac{e^{-ikl}}{\sqrt{l}}\sum_{n=0}^{\infty}\left[d(0,0)\frac{e^{-ikl}}{\sqrt{l}}\right]^{2n}, \qquad (26)$$

where p_0 is the pressure of the incident plane wave at $\mathbf{p}_1$. The first term of the infinite sum ($n=0$) is a single diffracted wave, that is, the incident plane wave diffracted once at point $\mathbf{p}_1$ before reaching $\mathbf{p}_2$. The second term ($n=1$) is a triple diffracted wave, that is, the incident plane wave first diffracted at point $\mathbf{p}_1$ and then diffracted at point $\mathbf{p}_2$, being again diffracted at point $\mathbf{p}_1$ before reaching $\mathbf{p}_2$. Other terms are for a greater number of round trips between $\mathbf{p}_1$ and $\mathbf{p}_2$. The diffracted pressure at point $\mathbf{r}$ is

$$p(\mathbf{r}) = p_2 d(\phi_2,\theta)\frac{e^{-ikr}}{\sqrt{r}} \qquad (27)$$

$$= p_0 d(\varphi,0)d(\phi_2,\theta)\frac{e^{-ikl}}{\sqrt{l}}\frac{e^{-ikr}}{\sqrt{r}}\sum_{n=0}^{\infty}\left[\left(d(0,0)\frac{e^{-ikl}}{\sqrt{l}}\right)^2\right]^n, \qquad (28)$$

where $d(\phi_2,\theta)e^{-ikr}/\sqrt{r}$ is the cylindrical acoustical wave from the corner $\mathbf{p}_2$ to the observation point $\mathbf{r}$. It is instructive to determine the energy $W(\mathbf{r}) = |p(\mathbf{r})|^2/2\rho c$ of this field. By squaring Eq. (28) and neglecting all cross-product terms, it yields

$$W(\mathbf{r}) = \frac{|p_0|^2}{2\rho c^2}|d(\varphi,0)|^2|d(\phi_2,\theta)|^2\frac{1}{lr}\sum_{n=0}^{\infty}\left[|d(0,0)|^2\frac{1}{l}\right]^{2n} \qquad (29)$$

$$= \frac{I_{\text{inc}}}{c}\frac{D_\omega(\varphi,0)D_\omega(\phi_2,\theta)}{1 - \dfrac{D_\omega^2(0,0)}{l^2}} \times \frac{1}{lr}, \qquad (30)$$

where $I_{\text{inc}}=|p_0|^2/2\rho c$ and $D_\omega=|d|^2$. The series converges when $D_\omega(0,0)/l < 1$. It is then apparent that GTD leads to the same energy field as predicted by Eq. (10) provided that all interferences between rays have been neglected. The set of Eqs. (5), (6), and (10) can thus be considered as an extension of geometrical acoustics in its strict sense, that is, with no phase attached to rays, which includes diffraction effects as done in GTD.

V. DIFFRACTION BY RECTANGLE

Consider a steady-state cylindrical wave of power ρ_0 diffracted by a rectangular obstacle of dimensions $a \times b$ as shown in Fig. 5. The incident wave is reflected on the front wall and diffracted by the four corners denoted by $\mathbf{p}_i$ with $i = 1, \ldots, 4$. Thus, the direct field is $\rho_0 G(\mathbf{s}, \mathbf{r})$ at any point $\mathbf{r}$
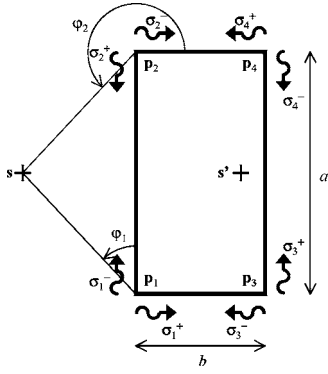
FIG. 5. Diffraction of a cylindrical wave emanating from **s** by a rectangle $a \times b$. Four fictitious sources of diffraction $\mathbf{p}_i$ are localized at the corners with powers $\sigma_i^\pm$ in grazing directions. The image source for reflected rays on the left side is **s'**.

and the reflected field is $\rho_0 G(\mathbf{s}', \mathbf{r})$ where **s'** is the image source given by reflection of **s** on the front wall.

At each diffracting corner is put a fictitious source $\sigma_i(\theta)$ whose particular values at angles $\theta = 0$ and $\theta = 3\pi/2$ are denoted σ_i^- and σ_i^+. Equations on $\sigma_i^\pm$ are obtained by applying Eq. (10). No reflected ray can be diffracted and therefore the second integral of Eq. (10) vanishes. Finally, $\sigma_i^\pm$ is only related to direct intensity $\rho_0 H(s)$ for points 1 and 2 and other values of $\sigma_j^\pm$,

$$\frac{\sigma_1^+}{2\pi} = \sigma_2^+ D_\omega\left(0, \frac{3\pi}{2}\right) H(a) + \sigma_3^- D_\omega\left(\frac{3\pi}{2}, \frac{3\pi}{2}\right) H(b)$$
$$+ \rho_0 D_\omega\left(\varphi_1, \frac{3\pi}{2}\right) H(s_1), \tag{31}$$

$$\frac{\sigma_1^-}{2\pi} = \sigma_2^+ D_\omega(0,0) H(a) + \sigma_3^- D_\omega\left(\frac{3\pi}{2}, 0\right) H(b)$$
$$+ \rho_0 D_\omega(\varphi_1, 0) H(s_1), \tag{32}$$

$$\frac{\sigma_2^+}{2\pi} = \sigma_1^- D_\omega\left(\frac{3\pi}{2}, \frac{3\pi}{2}\right) H(a) + \sigma_4^+ D_\omega\left(0, \frac{3\pi}{2}\right) H(b)$$
$$+ \rho_0 D_\omega\left(\varphi_2, \frac{3\pi}{2}\right) H(s_2), \tag{33}$$

$$\frac{\sigma_2^-}{2\pi} = \sigma_1^- D_\omega\left(\frac{3\pi}{2}, 0\right) H(a) + \sigma_4^+ D_\omega(0,0) H(b)$$
$$+ \rho_0 D_\omega(\varphi_2, 0) H(s_2), \tag{34}$$

$$\frac{\sigma_3^+}{2\pi} = \sigma_1^+ D_\omega\left(0, \frac{3\pi}{2}\right) H(b) + \sigma_4^- D_\omega\left(\frac{3\pi}{2}, \frac{3\pi}{2}\right) H(a), \tag{35}$$

$$\frac{\sigma_3^-}{2\pi} = \sigma_1^+ D_\omega(0,0) H(b) + \sigma_4^- D_\omega\left(\frac{3\pi}{2}, 0\right) H(a), \tag{36}$$

$$\frac{\sigma_4^+}{2\pi} = \sigma_2^- D_\omega\left(\frac{3\pi}{2}, \frac{3\pi}{2}\right) H(b) + \sigma_3^+ D_\omega\left(0, \frac{3\pi}{2}\right) H(a), \tag{37}$$

$$\frac{\sigma_4^-}{2\pi} = \sigma_3^+ D_\omega(0,0) H(a) + \sigma_2^- D_\omega\left(\frac{3\pi}{2}, 0\right) H(b), \tag{38}$$

where s_1, s_2, φ_1, and φ_2 are defined in Fig. 5. This is a set of linear equations on the eight unknowns $\sigma_i^\pm$. Furthermore, the potential σ_i in all other directions θ is also given by Eq. (10),

$$\frac{\sigma_1(\theta)}{2\pi} = \sigma_2^+ D_\omega(0, \theta) H(a) + \sigma_3^- D_\omega\left(\frac{3\pi}{2}, \theta\right) H(b)$$
$$+ \rho_0 D_\omega(\varphi_1, \theta) H(s_1), \tag{39}$$

$$\frac{\sigma_2(\theta)}{2\pi} = \sigma_1^- D_\omega\left(\frac{3\pi}{2}, \theta\right) H(a) + \sigma_4^+ D_\omega(0, \theta) H(b)$$
$$+ \rho_0 D_\omega(\varphi_2, \theta) H(s_2), \tag{40}$$

$$\frac{\sigma_3(\theta)}{2\pi} = \sigma_1^+ D_\omega(0, \theta) H(b) + \sigma_4^- D_\omega\left(\frac{3\pi}{2}, \theta\right) H(a), \tag{41}$$

$$\frac{\sigma_4(\theta)}{2\pi} = \sigma_2^- D_\omega\left(\frac{3\pi}{2}, \theta\right) H(b) + \sigma_3^+ D_\omega(0, \omega) H(a). \tag{42}$$

Thus, the functions $\sigma_i(\theta)$ are well defined by the particular values $\sigma_i^\pm$.

Finally, the field at any point **r** is given by adding the contributions of the direct field, the reflected field and the four diffracted fields. It yields

$$W(\mathbf{r}) = \rho_0 G(\mathbf{s}, \mathbf{r}) + \rho_0 G(\mathbf{s}', \mathbf{r}) + \sum_{i=1}^{4} \sigma_i(\theta_i) G(\mathbf{p}_i, \mathbf{r}), \tag{43}$$

$$\mathbf{I}(\mathbf{r}) = \rho_0 \mathbf{H}(\mathbf{s}, \mathbf{r}) + \rho_0 \mathbf{H}(\mathbf{s}', \mathbf{r}) + \sum_{i=1}^{4} \sigma_i(\theta_i) \mathbf{H}(\mathbf{p}_i, \mathbf{r}), \tag{44}$$

where θ_i is the emission angle at point $\mathbf{p}_i$ toward **r**. Remember that only some of the six fields can reach the point **r** depending on its position, the others being stopped by the obstacle.

Two numerical simulations are proposed in Figs. 6 and 7. The size of the rectangle is 10 m × 2 m and the source point is located at a distance of 4 m on the left of the rectangle and on the middle axis. In Fig. 6, the frequency range of the sound source is the third octave band centered on 250 Hz, and the wavelength of sound is about 1.4 m, which is not very different from the smaller dimension of the diffracting object. In Fig. 7, the frequency range of the sound source is the third octave band centered on 5000 Hz, and the wavelength of sound is about 0.07 m, which is very small with regards to the size of the diffracting object. For both cases, two results are provided, on the one hand the SPL from Eq. (43) is plotted at the centered frequency and on the other hand, the BEM is employed. For BEM studies, calculations are performed every 25 Hz for the third-octave band centered on 5000 Hz and every 5 Hz for the third-octave band centered on 250 Hz, and the final result is the quadratic average of these, or, in other words, is the rms value.

For both cases, the transfer equation leads to infinite results in the vicinity of the boundaries between illuminated and shadow zones. These boundaries are visible on the SPL
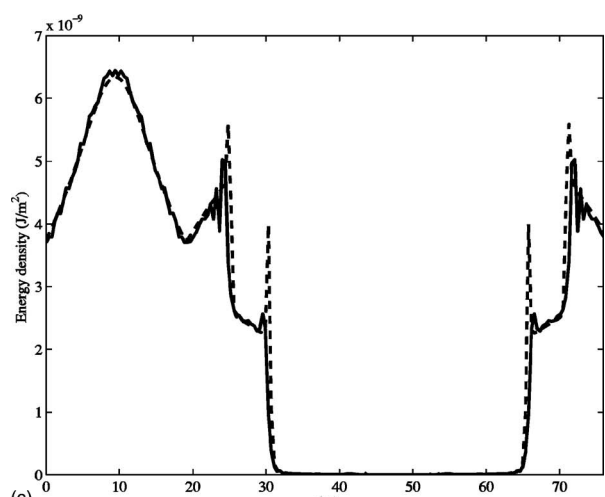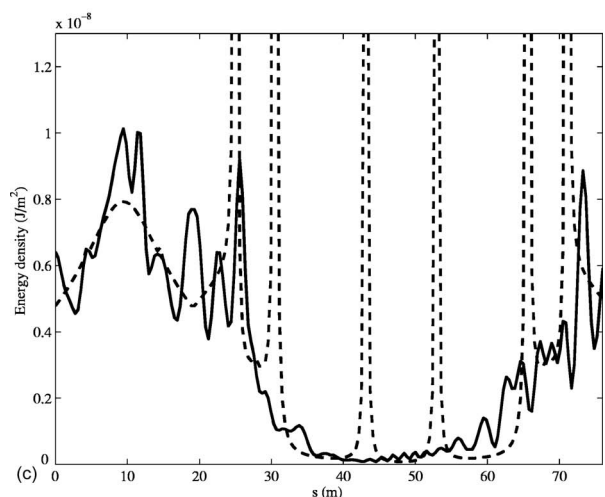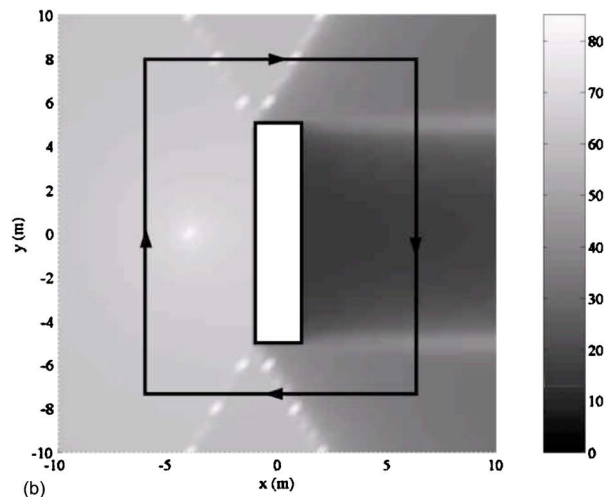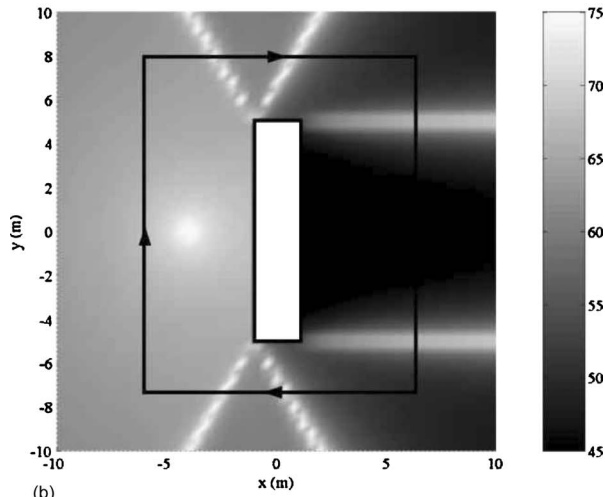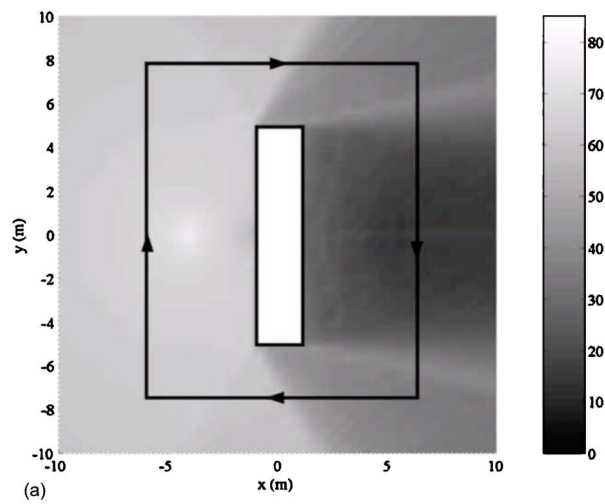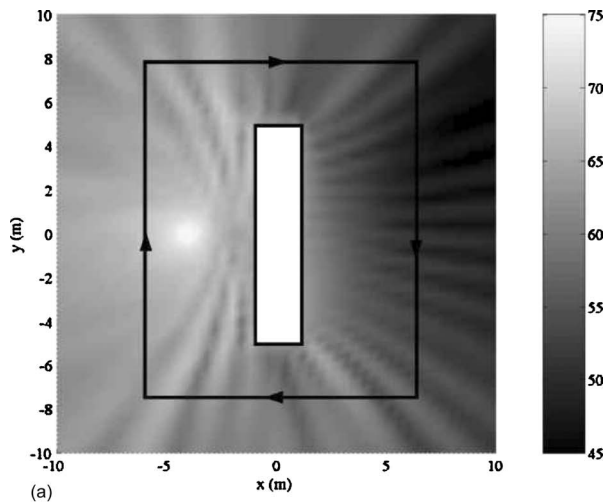
FIG. 6. Diffraction of a cylindrical wave by a rectangular obstacle (10 m ×2 m). SPL in dB around the obstacle predicted by (a) the boundary element method and (b) the transfer equation. (c) Energy density along the contour line beginning at the left bottom corner, with the boundary element method (—) and with the transfer equation (---). The frequency is 250 Hz.

FIG. 7. Diffraction of a cylindrical wave by a rectangular obstacle (10 m ×2 m). SPL in dB around the obstacle predicted by (a) the boundary element method and (b) the transfer equation. (c) Energy density along the contour line beginning at the left bottom corner, with the boundary element method (—) and with the transfer equation (---). The frequency is 5000 Hz.

map in Fig. 6(b) and in Fig. 7(b) and where they appear as white areas. Oblique boundaries correspond to the limit of influence of direct and reflected fields while others correspond to the limit of influence of fields diffracted by the opposite corner. It is well known that in the vicinity of these

boundaries the acoustical field cannot be developed in terms of rays. This is the same limitation as encountered in GTD since the diffraction coefficient implemented in this calculation is the one of GTD.

The main difference between the result given by the BEM and the result from the transfer equation is that the

fluctuations due to the existence of some remaining interferences are noticeable on the BEM result, while they do not appear on the result from the transfer equation which is based on the assumption that direct, reflected, and diffracted waves are uncorrelated. These interferences have a major effect when the wavelength of sound is close to the size of the diffracting object as shown in Fig. 6(a), and in this case, the result given by the transfer equation only represents the average behavior of the acoustical field around the rectangle [Fig. 6(c)]. However, when the frequency increases, or more generally, when the ratio between the wavelength and the size of the diffracting object decreases, the effect of interferences vanishes and, thus, both methods well agree as shown in Figs. 7(a)–7(c).

VI. DISCUSSION

One of the main advantages of the radiative transfer method for the prediction of sound fields is that computation times are significantly reduced compared to some other methods such as the BEM. The calculations absolutely do not depend on the wavelength of sound if parameters such as atmospheric or material absorption coefficients do not depend on frequency. Otherwise, the variations of these parameters define the frequency step to use in order to apply the method. Thus, in the case of diffraction, the energetic diffraction coefficient depends on frequency: the magnitude of the diffraction coefficient introduced in GTD decreases like $1/\sqrt{k}$ so the energetic diffraction coefficient decreases like $1/k$, where k is the wave number. The allowed frequency bandwidth for the study depends on the frequency variations of the energetic diffraction coefficient: the frequency step is chosen so that the diffraction coefficient does not vary much on the bandwith. Thus, the change in the nature of the acoustical field will be well described by the radiative transfer method, except for interference effects. However, as any ray approach, this method cannot give accurate results for low frequencies where the wavelength is of the same order as the typical length of the problem. In such cases, wave-based approaches should be employed. For instance, the typical lengths for the example of Sec. III (Figs. 1 and 3) are the source-edge and edge-receiver distances. Ray theory then applies provided that these distances are larger than one wavelength beyond the near-field influence. In the example of Sec. IV (Fig. 4), the distance between the two diffracting lines must also be larger than one wavelength whereas in the example of Sec. V (Figs. 5 and 7) length and width of the rectangle must respect the same criteria. The method would fail for arbitrarily small diffracting objects (Fig. 6).

VII. CONCLUSION

In this paper, it has been proposed to apply the radiative transfer approach to diffraction. The functional equation (10) gives the power of fictitious sources of diffraction. The interest of such an equation is to determine the total diffracted power in any direction. All well-known results on diffraction by wedges in the frame of GTD are recovered. Equation (10) leads to a set of linear equations. By solving this system, it is possible to determine the total diffracted power by corners, without following the rays as is usually done with the ray-tracing technique.

The method has two main limitations. First, some unphysical results are obtained in the vicinity of boundaries between illuminated and shadow zones. This is the same limitation as in GTD for same reason. Second, interference effects cannot be described by the present method because energies are added. This is an additional limitation which does not occur in GTD.

Compared with BEM this method is CPU-time saving. BEM is limited in practice to low frequencies. In the high frequency range, the number of fictitious sources introduced on the mesh is rapidly prohibitive in regard to current computers. On the other hand, the number of fictitious sources required in the transfer equation (10) does not depend on the frequency, which leads to a constant CPU time at any frequency. This provides an alternative method in the field of high frequency diffraction.

Furthermore, this approach is better suited than GTD to the case of multiple diffraction. All orders of diffraction are simultaneously taken into account and thus, in practice, results are more accurate than using GTD where a limited number of rays are used. Besides, it does not require the knowledge of all ray paths between the source and the receiver point which can be tedious to determine in practice.

APPENDIX

This Appendix concerns the evaluation of the energetic diffraction coefficient D_ω. Consider an incident ray in the direction $\mathbf{v} = \varphi, \beta$ impinging on a wedge at point $\mathbf{q}$. The diffracted field at any point $\mathbf{r}$ in the direction $\mathbf{u} = \theta, \alpha$ is given by

$$p_{\text{dif}}(\mathbf{r}) = p_{\text{inc}}(\mathbf{q}) d_\alpha(\varphi, \theta) \frac{e^{-ikR}}{\sqrt{R}}, \tag{A1}$$

where k is the wave number, $p_{\text{inc}}(\mathbf{q})$ is the incident field at the diffraction point $\mathbf{q}$, and $R = |\mathbf{q} - \mathbf{r}|$ is the distance measured along the diffracted ray. The diffraction coefficient d_α depends on φ and θ the incidence and emission directions defined to the right side of the wedge (Fig. 1) and also on the outer angle of the wedge ϕ by means of the wedge index $\nu = \pi/\phi$. According to Keller's law of diffraction[1] the angle of diffraction α equals the angle of incidence β so that the diffracted rays emanating from $\mathbf{q}$ belong to a cone whose axis is the diffracting edge. An expression for d_α is derived using the method of steepest descent,[2,4]

$$d_\alpha(\varphi,\theta) = \frac{e^{-i\pi/4}\nu\sin(\nu\pi)}{\sqrt{2\pi k \sin\alpha}}\left[\frac{1}{\cos(\nu\pi)-\cos[\nu(\theta+\varphi)]}\right.$$

$$\left. + \frac{1}{\cos(\nu\pi)-\cos[\nu(\theta-\varphi)]}\right]. \tag{A2}$$

d_α becomes singular on incidence or reflection boundaries. This coefficient depends on the frequency through the wave number k.

The diffracted intensity $I_{\text{dif}}(\mathbf{r}) = |p_{\text{dif}}|^2/2\rho c$ where c is the sound speed, ρ is the fluid density, is from Eq. (A1)

$$I_{\text{diff}}(\mathbf{r}) = \frac{I_{\text{inc}}(\mathbf{q})}{R}|d_\alpha(\varphi,\theta)|^2, \tag{A3}$$

with $I_{\text{inc}}(\mathbf{q}) = |p_{\text{inc}}(\mathbf{q})|^2/2\rho c$ the incident intensity. By denoting $r = R\sin\alpha$ the edge-receiver distance, Eq. (A3) is written by means of the diffraction coefficient $d(\varphi,\theta)$ at normal incidence $\alpha = \pi/2$,

$$I_{\text{dif}}(\mathbf{r}) = \frac{I_{\text{inc}}(\mathbf{q})}{r}|d(\varphi,\theta)|^2. \tag{A4}$$

By comparing with Eq. (18) and noting that $I_{\text{dif}} = cW_{\text{dif}}$, it is readily found that $D_\omega(\varphi,\theta) = |d(\varphi,\theta)|^2$. This is the energetic diffraction coefficient at normal incidence.

[1]J. B. Keller, "Geometrical theory of diffraction," J. Opt. Soc. Am. **62**, 116–130 (1962).

[2]A. D. Pierce, *Acoustics—An Introduction to Its Physical Principles and Applications*, 2nd printing (Acoustical Society of America, American Institute of Physics, New York, 1991).

[3]W. J. Hadden and A. D. Pierce, "Sound diffraction around screens and wedges for arbitrary point source locations," J. Acoust. Soc. Am. **71**, 1290 (1982).

[4]A. D. Pierce, "Diffraction around corners and over barriers," J. Acoust. Soc. Am. **55**, 941–955 (1974).

[5]U. J. Kurze, "Noise reduction by barriers," J. Acoust. Soc. Am. **55**, 504–518 (1974).

[6]H. Medwin, E. Childs, and G. M. Jebsen, "Impulse studies of double diffraction: A discrete Huyghens interpretation," J. Acoust. Soc. Am. **72**, 1005–1013 (1982).

[7]D. Ouis, "Noise attenuation by a hard wedge-shaped barrier," J. Sound Vib. **262**, 347–364 (2003).

[8]B. J. Jin, H. S. Kim, H. J. Kang, and J. S. Kim, "Sound diffraction by a partially inclined noise barrier," Appl. Acoust. **62**, 1107–1121 (2001).

[9]R. G. Kouyoumjian and P. H. Pathak, "A uniform geometrical theory of diffraction for an edge in a perfectly conducting surface," Proc. IEEE **62**, 1448–1461 (1974).

[10]M. F. Modest, *Radiative Heat Transfer* (McGraw-Hill, New York, 1993).

[11]H. Kuttruff, *Room Acoustics*, 3rd ed. (Elsevier Applied Science, London, 1991).

[12]M. Carroll and C. Chien, "Decay of reverberent sound in a spherical enclosure," J. Acoust. Soc. Am. **62**, 1442–1446 (1977).

[13]R. Miles, "Sound field in a rectangular enclosure with diffusely reflecting boundaries," J. Sound Vib. **92**, 203–226 (1984).

[14]H. Kuttruff, "Energetic sound propagation in rooms," Acust. Acta Acust. **83**, 622–628 (1997).

[15]A. Le Bot and A. Bocquillet, "Comparison of an integral equation on energy and the ray-tracing technique for room acoustics," J. Acoust. Soc. Am. **108**, 1732–1740 (2000).

[16]A. Le Bot, "Energy transfer for high frequencies in built-up structures," J. Sound Vib. **250**, 247–275 (2002).

[17]V. Cotoni and A. Le Bot, "Radiation of plane structures at high frequency using an energy method," Int. J. Acoust. Vib. **6**, 209–214 (2001).

[18]L. P. Franzoni, D. B. Bliss, and J. W. House, "An acoustic boundary element method based on energy and intensity variables for prediction of high frequency broadband sound fields," J. Acoust. Soc. Am. **110**, 3071–3080 (2001).

[19]A. Wang, N. Vlahopoulos, and K. Wu, "Development of an energy boundary element formulation for computing high-frequency sound radiation from incoherent intensity boundary conditions," J. Sound Vib. **278**, 413–436 (2004).

[20]E. Reboul, A. Le Bot, and J. Perret-Liaudet, "Introduction of acoustical diffraction in the radiative transfer method," C. R. Mec. **332**, 505–511 (2004).

[21]A. Le Bot, "A functional equation for the specular reflection of rays," J. Acoust. Soc. Am. **112**, 1276–1287 (2002).

[22]W. Joyce, "Sabine's reverberation time and ergodic auditoriums," J. Acoust. Soc. Am. **58**, 643–655 (1975).